JOURNAL OF MAGNETIC RESONANCE **125,** 132–139 (1997)
ARTICLE NO. MN961087

REPULSION, A Novel Approach to Efficient Powder Averaging in Solid-State NMR

MADS BAK AND NIELS CHR. NIELSEN

Department of Chemistry, University of Aarhus, DK-8000 Aarhus C, Denmark

Received November 12, 1996

A novel approach to efficient powder averaging in magnetic resonance is presented. The method relies on a simple numerical procedure which based on a random set of crystallite orientations through simulation of fictive intercrystallite repulsive forces iteratively determines a set of orientations uniformly distributed over the unit sphere. The so-called REPULSION partition scheme is compared to earlier methods with respect to the distribution of crystallite orientations, solid angles, and powder averaging efficiency. It is demonstrated that powder averaging using REPULSION converges faster than previous methods with respect to the number of crystallite orientations involved in the averaging. This feature renders REPULSION particularly attractive for calculation of magic-angle-spinning solid-state NMR spectra using a minimum of crystallite orientations. For numerical simulation of powder spectra, the reduced number of required crystallite orientations translates into shorter computation times and simulations less prone to systematic errors induced by finite sets of nonuniformly distributed crystallite orientations.

INTRODUCTION

An important ingredient to the success of solid-state NMR as a probe to detailed information on the structure and dynamics of solids is the ability to perform accurate simulation and iterative fitting of experimental spectra. Optimum simulated spectra may be regarded representatives for structural and dynamical parameters of the nuclear spin Hamiltonian which in many cases are not extractable solely by visual inspection of experimental spectra. This is particularly true when operating with powder samples, which often may be desirable either because this type of sample is the easiest to obtain and handle experimentally or because sufficiently large single crystals cannot be produced.

Simulation of solid-state NMR powder spectra requires integration over all randomly distributed crystallite orientations. Since it is difficult or impossible to perform this integration by analytical means, powder averaging is usually accomplished numerically by performing a weighted sum of single-crystal spectra representing a large set of crystallite orientations ideally being uniformly distributed over the unit sphere. Because the computation time is proportional to the number of crystallite orientations *and* because high-quality averaging corresponding to a uniform distribution of crystallite orientations is critical for obtaining reliable parameters for anisotropic parts of the spin Hamiltonian, several studies have recently addressed methods for efficient powder averaging in magnetic resonance (*1–5*).

A criterion for, in a minimum number of steps, achieving acceptable powder averaging corresponding to a uniform distribution of crystallite orientations, is that each orientation through its weighting factor contributes equally to the sum of contributions from all crystallites. Otherwise, expensive computing time is spent on crystallites only providing a minor contribution to the spectrum. Since each weighting factor may be assumed proportional to the solid angle, this criterion may be regarded equivalent to finding the most uniform distribution of crystallite orientations over the unit sphere. Despite numerous studies it has not, to our knowledge, been demonstrated possible to derive a set of truly uniformly distributed crystallite orientations by analytical means. In this work, we introduce a simple numerical method for deriving sets of uniformly distributed crystallite orientations and evaluate its usefulness for calculation of solid-state NMR powder spectra using a minimum number of crystallites.

POWDER AVERAGING

In general, the free-induction decay observed for a powder may be described by

$$s(t) = \frac{1}{8\pi^2}\int_0^{2\pi} d\alpha \int_0^{\pi} d\beta \sin(\beta) \int_0^{2\pi} d\gamma s(t; \alpha, \beta, \gamma), \quad [1]$$

where $s(t; \alpha, \beta, \gamma)$ characterizes the time evolution of a single crystal with an orientation relative to the laboratory reference frame specified by the Euler angles (α, β, γ) (*6, 7*). In the context of solid-state NMR, the dependence

1090-7807/97 $25.00

TABLE 1
Euler Angles and Weighting Factors for Various Powder-Averaging Methods Routinely Applied for Calculation of Solid-State NMR Spectra[a]

	M	α_{ij}	β_{ij}	w_{ij}
Planar random	1	$\in[0, 2\pi[$	$\in[0, \pi[$	$\sin(\beta_{ij})$
Spherical random	1	$\in[0, 2\pi[$	$\cos(\beta_{ij}) \in [0, 1[$	1
Planar grid	M	$2\pi \frac{i-1}{N}$	$\pi \frac{j}{M+1}$	$\sin(\beta_{ij})$
Spherical grid	M	$2\pi \frac{i-1}{N}$	$\cos^{-1}\left(1 - \frac{2j}{M+1}\right)$	1
Planar ZCW[b]	1	$2\pi\ Frac\left[\frac{i-1}{N} g_1\right]$	$\pi\ Frac\left[\frac{i-1}{N} g_2\right]$	$\sin(\beta_{ij})$
Spherical ZCW[b]	1	$2\pi\ Frac\left[\frac{i-1}{N} g_1\right]$	$\cos^{-1}\left(1 - 2Frac\left[\frac{i-1}{N} g_2\right]\right)$	1
Alderman[c]	N − i	$\tan^{-1}\left(\frac{j}{i}\right)$	$\cos^{-1}\left(\frac{N-i-j}{R_{ij}}\right)$	$\left(\frac{N}{R_{ij}}\right)^3$
SOPHE[d]	i	$\frac{\pi}{2}\frac{i-j+1}{i}$	$\frac{\pi}{2}\frac{i}{N-1}$	1

[a] The integers i, j, N, and M correspond to the powder averaging scheme of Eq. [3].
[b] *Frac* is a function that returns the fractional part of the argument. g_1 and g_2 may be selected according to Refs. (*9, 10*).
[c] $R_{ij} = \sqrt{i^2 + j^2 + (N - i - j)^2}$. First octant only; the remaining seven octants are related to the first octant by symmetry (*1*).
[d] N replaced by N − 1 in Eq. [3]. In the present study, the weighting factor is calculated using Eq. [9].

on γ may often be treated separately. For static samples, γ represents an immaterial rotation about the external magnetic field axis. For rotating samples, γ describes a rotation about the rotor axis conveniently being factored into the angle describing the rotor revolution. In both cases, this effectively leaves us with

$$s(t) = \frac{1}{4\pi}\int_0^{2\pi} d\alpha \int_0^{\pi} d\beta \sin(\beta)\, s(t; \alpha, \beta), \qquad [2]$$

depending only on two variables. In practice, Eq. [2] is approximated by the sum

$$s(t) = \sum_{i=1}^{N}\sum_{j=1}^{M} s(t; \alpha_{ij}, \beta_{ij}) w_{ij}, \qquad [3]$$

where we introduced the subscript *ij* indicating that the Euler angles may depend on two indices *i* and *j* not necessarily being selected independently. w_{ij} denotes the crystallite weights normalized according to $\sum_{i=1}^{N}\sum_{j=1}^{M} w_{ij} = 1$.

Several powder-averaging methods have been proposed for calculation of solid-state NMR spectra. Table 1 gives formulas for Euler angles and weighting factors applied for random selection of Euler angles, two-dimensional grids, the method of Zaremba (*8*), Conroy (*9*), and Wolfsberg and co-workers (*10*) (henceforth referred to as ZCW), the method of Alderman *et al.* (*1*), and the more recent SOPHE method (*5*). These formulas provide the basis for a graphical demonstration of the distribution of crystallite orientations for the different methods and for comparison of their powder-averaging efficiency through specific calculation of solid-state NMR spectra. We note that our comparison only concerns the performance in regards to the selection of the crystallite orientations, whereas the potential of the methods when combined with interpolation is not evaluated.

An impression of the various partition algorithms may be obtained from the two- and three-dimensional plots in Fig. 1 showing the distribution of about 150 crystallites over the 2D α, β plane as well as over the 3D surface of the unit sphere. It is evident that random selection leads to a rather nonuniform distribution of the crystallites and thereby inefficient powder averaging. More uniform distributions are obtained using the various methods for systematic selection of the crystallite orientations. It is noted that the planar random, grid, and ZCW methods, aiming at a uniform distribution of crystallites in the α, β 2D plane, leads to a relatively high density of crystallites near the poles. To compensate for this, each contribution is weighted by $w_{ij} = \sin(\beta_{ij})$. This seemingly unfavorable weighting (*vide infra*) is avoided in the corresponding spherical methods evaluating $\cos(\beta)$ instead of β. We note that the ZCW partition scheme (*8–10*) (Figs. 1d and 1e) recently has attracted considerable interest as a very efficient powder-aver-

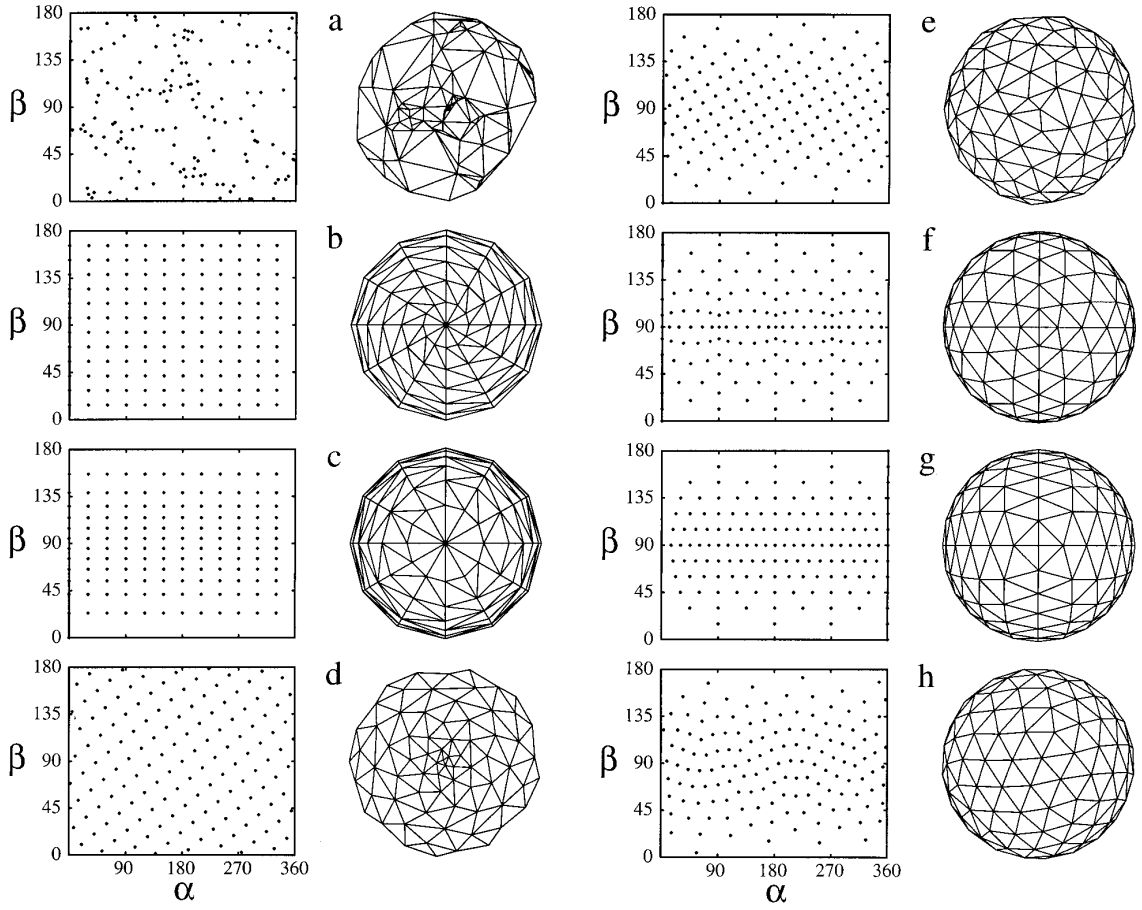

FIG. 1. Planar (left) and spherical (right) representations of crystallite orientations for powder-averaging methods employing (a) 150 random, (b) 144 planar grid, (c) 144 spherical grid, (d) 143 planar ZCW, (e) 143 spherical ZCW, (f) 145 Alderman, (g) 146 SOPHE, and (h) 144 REPULSION crystallites (see text). It is noted that (a, b, d) and (c, e–h) originate from methods striving at uniform distribution of crystallite orientations within the α, β 2D plane and over the 3D unit sphere, respectively.

aging method (*4*). Optimum powder-averaging efficiency using this method ideally requires adjustment of the g_1 and g_2 values (see Table 1) to the function for which the powder averaging must be performed (*4, 10*). Since such optimization may be impractical, for example, in case of iterative fitting involving variation of parameters causing significant functional changes, we restrict ourselves to the g values given by Cheng *et al.* (*10*) for the two-dimensional function $f = \alpha^2\beta^2$ and by Koons *et al.* (*4*) for the anisotropic chemical shielding function. Similarities between calculations of powder spectra performed using partition schemes optimized to these widely different functions confirm that the g values given by Conroy (*9*) and Cheng *et al.* (*10*) may be regarded generally applicable (*4*).

THE REPULSION METHOD

Figure 1 indicates difficulties in obtaining a set of crystallite orientations uniformly distributed over the unit sphere by analytical means. To solve this problem, we instead adapt a simple numerical approach to derive uniformly distributed sets of crystallite orientations for fast and reliable powder averaging using a minimum number of crystallites. Realization of equal solid angles for a given number of points on a spherical surface corresponds to establishing the set of points for which each point exhibits the largest possible distance to all neighboring points. Physically, this situation would, for example, occur for the equilibrium state of a system of particles on a spherical surface subjected only to interparticle repulsive forces. The repulsive force could, for example, be inversely proportional to the square of the surface distance between the points similar to the case of Coulomb repulsion between particles of equal charge. This example represents the basis for our so-called REPULSION method where the equilibrium state is determined iteratively by moving the particles under influence of the repulsive forces from the other particles on the surface. When the

system reaches equilibrium, the particles are distributed with maximum distance to each other.

Consider N particles randomly distributed on a spherical surface. Let O be origin and P_k the coordinates of particle k on the unit sphere. Upon introducing a repulsive force between the particles i and j, the two particles will separate along the direction

$$\overrightarrow{dP_{ij}} = (\overrightarrow{OP_j} \times \overrightarrow{OP_i}) \times \overrightarrow{OP_i}, \qquad [4]$$

provided the displacement for each particle is sufficiently small that movement along the tangent to a good approximation corresponds to that on the spherical surface. Within this assumption, repulsion between N particles would cause particle i to move to the position

$$\overrightarrow{OP}_i^{\text{new}} = \frac{\overrightarrow{OP}_i^{\text{old}} + \overrightarrow{dP_i}}{|\overrightarrow{OP}_i^{\text{old}} + \overrightarrow{dP_i}|} \qquad [5]$$

with the total displacement of particle i being defined as

$$\overrightarrow{dP_i} = C \sum_{j \neq i} \frac{1}{\vartheta_{ij}^2} \frac{\overrightarrow{dP_{ij}}}{|\overrightarrow{dP_{ij}}|}. \qquad [6]$$

In Eq. [6], C is a scaling factor ensuring all displacements to be sufficiently small and ϑ_{ij} is the angle between the vectors $\overrightarrow{OP_i}$ and $\overrightarrow{OP_j}$,

$$\vartheta_{ij} = \cos^{-1}(\overrightarrow{OP_i} \cdot \overrightarrow{OP_j}), \qquad [7]$$

to which the surface distance is proportional. Using Eqs. [4]–[7], it is straightforward to set up a procedure which based on any (e.g., random) set of crystallite orientations iteratively determines the equilibrium state corresponding to the maximum separation between all points. For each step of the iteration, the displacements for all points are calculated using an appropriate value of C to ensure smooth convergence. Then all particles are made to move instantaneously. This procedure is repeated until convergence after which the Cartesian coordinates are converted to Euler angles using $x = \sin(\beta)\cos(\alpha)$, $y = \sin(\beta)\sin(\alpha)$, and $z = \cos(\beta)$. For the convenience of the reader, Appendix 1 contains a pseudo computer code specifying our procedure for derivation of REPULSION Euler angles for any desired number of crystallites N.

Generally, the very simple procedure outlined in Appendix 1 converges within about 1000 iterations employing realistic values of N up to about 1000. On a SUN Sparc 10/50 workstation, this corresponds to processing times of about 2 and 30 m for N values of 144 and 1000, respectively. We note that attempts to change the distance dependence of the repulsion from the square dependence assumed above to other factors in the exponent leads to sets of crystallite orientations of similar quality, although the number of iterations required for convergence depends on this exponent. It is also noted that similar sets of Euler angles alternatively may be calculated using nonlinear optimization (*11*) to minimize $\Sigma_{i \neq j} \vartheta_{ij}^{-2}$, however, at the expense of severely prolonged computing times.

The distribution of crystallites over the α, β 2D plane and the 3D spherical surface corresponding to REPULSION averaging using $N = 144$ crystallite orientations is illustrated in Fig. 1h. Clearly, relative to state-of-the-art methods, REPULSION provides a very uniform distribution of crystallites over the unit sphere. This implies that all weighting factors intuitively may be assumed equal. In practice, this proves to be a good approximation, although slightly better performance may be obtained using a refined set of weighting factors taking into account minor variations in the crystallite solid angles. A first indication of small variations in the solid angles becomes apparent by counting the number of closest neighbors to each crystallite (corresponding to the number of lines extending from each point in Fig. 1h). It appears that, although the vast majority of crystallites have six neighbors, there will always be a small fraction of crystallites having five and/or seven neighbors depending on the total number of crystallites. Since each crystallite orientation is defined through its repulsion to all other crystallites, it is tempting to relate the weighting factor of each crystallite to its repulsion to the surrounding crystallites. Thus, if the effective area (i.e., the solid angle) for a given crystallite i is assumed inversely proportional by some order b to its repulsion to all other crystallites, we may define a refined weighting factor by

$$w_{ij} \propto \left(\sum_{k \neq i} (\vartheta_{ik})^{-2}\right)^{-b}, \qquad [8]$$

with $k = 1, \ldots, N$ and $j = 1$. In our experience, $b = 3$ provides the most efficient powder averaging.

EVALUATION OF POWDER AVERAGING

To compare the effective weighting factors for the different methods, we employ a simple pictorial approach to numerically calculate and display the solid angle associated with each crystallite orientation without assuming any system in the generation of these orientations. The ''solid angle'' of a point may be approximated by the area on the unit sphere being closer to that point than to its neighbors. A neighbor to a given point on the unit sphere is defined as a point to which a line can be drawn (on the surface) that is shorter than all other lines crossing it. These lines correspond exactly to those forming the spherical plots in Fig. 1. By inserting fictive points at the half distance between all neigh-

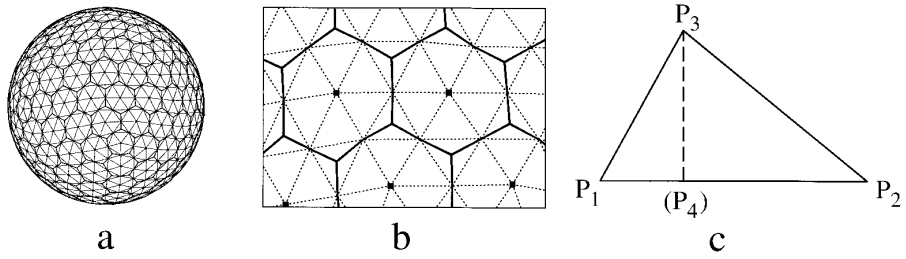

FIG. 2. (a, b) Graphical illustration of the area (i.e., the solid angle) on the spherical surface corresponding to each crystallite point (specifically the points corresponds to REPULSION with 168 crystallite orientations). The bounded areas (solid line) is formed by connecting fictive points taken at the half distance between the crystallite itself and its closest neighbors and subsequently sharing the areas of the triangles not containing any crystallite point among the three closest crystallite points. (c) Definition of points P_1, P_2, P_3, and P_4 for any triangle on the surface of the unit sphere employed for calculation of the surface area (solid angle) corresponding to each crystallite orientation (see text).

boring points and connecting points surrounding a given crystallite, the main part of the area constituting the solid angle is bounded. The areas of the remaining triangles also generated through this partition of the unit sphere are distributed equally to the three surrounding crystallite areas. As illustrated for specific regions of the unit sphere for a set of REPULSION crystallites in Figs. 2a and 2b, this procedure leads to well-defined areas (bounded by solid lines), enabling visualization of the solid angle and thereby the weighting factor corresponding to any crystallite orientation on the unit sphere. The distribution and the variation of the solid angles for the various powder-averaging methods are illustrated by 3D spherical plots in Fig. 3. This representation demonstrates significant variation in the effective solid angles for the various methods and reinforces the impression that REPULSION exhibits the most uniform distribution of crystallite orientations.

The solid angles represented graphically in Fig. 3 may be evaluated numerically by calculating the area of all triangles constituting the bounded areas according to Fig. 2. Specifically, the area of a triangle on the unit sphere spanned by the points P_1, P_2, and P_3 sorted such that $\vartheta_{12} \geq \vartheta_{13}, \vartheta_{23}$ (Fig. 2c) may be calculated using the following simple procedure. First, a projection point P_4 on the spherical surface (see Fig. 2c) is generated by calculating the projection $\overrightarrow{P_1P_4}$ of $\overrightarrow{P_1P_3}$ onto $\overrightarrow{P_1P_2}$ and defining $\overrightarrow{OP_4}$ as the normalized variant of the vector $\overrightarrow{OP_1} + \overrightarrow{P_1P_4}$. Then the triangle is reconstructed with the same surface distances but with P_1, P_2, and P_4 located at the equator of the unit sphere. This facilitates calculation of the areas of the two triangles $P_1P_3P_4$ and $P_4P_3P_2$ to simple surface integrals depending on α and β. Using this procedure, the area of the full triangle $P_1P_3P_4$ may be expressed by

$$\text{Area}_{123} = \frac{\vartheta_{12}}{\vartheta_{34}}\,[1 - \cos(\vartheta_{34})]. \qquad [9]$$

Using Eq. [9] and adding contributions from all triangles constituting each crystallite area, the various powder-averaging methods may conveniently be characterized by plots displaying the solid angles sorted according to size against the crystallite number as illustrated in the right-hand columns of Fig. 4. For comparison, the left-hand columns

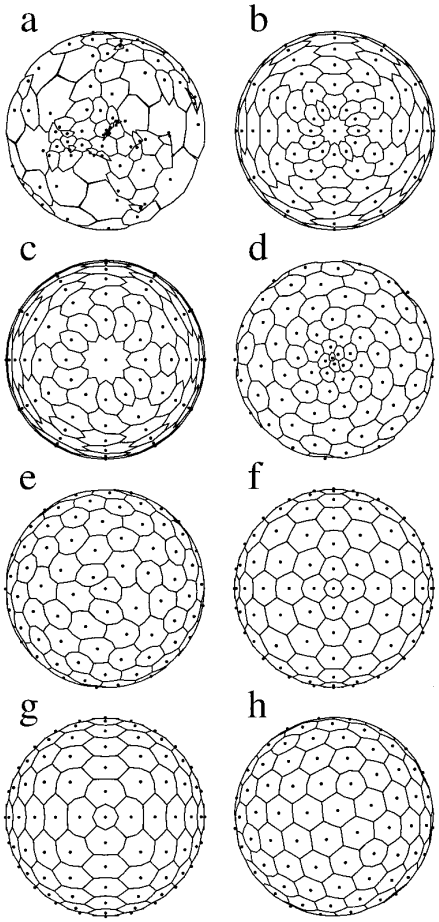

FIG. 3. Spherical plots of the areas closest to each crystallite (i.e., the solid angles) obtained using the procedure described in the text for (a) 150 random, (b) 144 planar grid, (c) 144 spherical grid, (d) 143 planar ZCW, (e) 143 spherical ZCW, (f) 145 Alderman, (g) 146 SOPHE, and (h) 144 REPULSION crystallites.

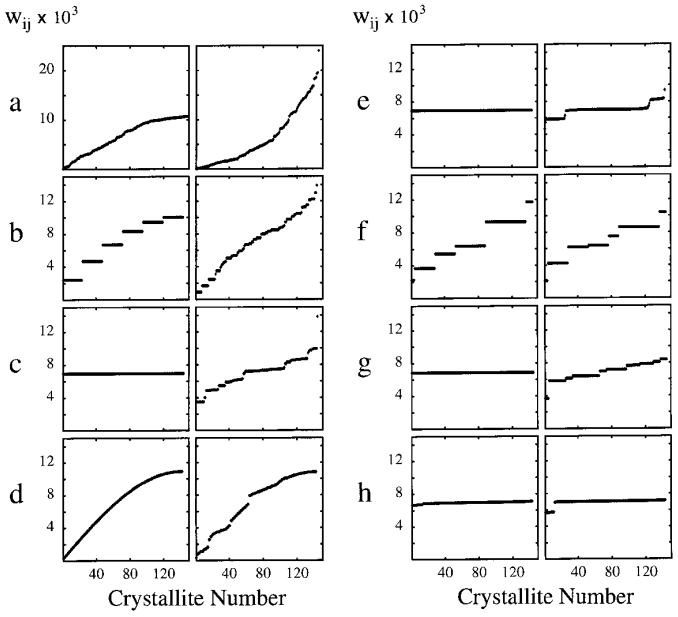

FIG. 4. Sorted weighting factors (left) and solid angles (right) for the crystallites associated with powder averaging using (a) 150 random, (b) 144 planar grid, (c) 144 spherical grid, (d) 143 planar ZCW, (e) 143 spherical ZCW, (f) 145 Alderman, (g) 146 SOPHE, and (h) 144 REPULSION crystallites. The weighting factors are those recommended for each method, apart from the SOPHE method where unit factors are shown. For the REPULSION method, the weighting factors were generated using Eq. [8]. All solid angles were calculated using Eq. [9].

of Fig. 4 include corresponding plots of the weighting factors actually used in the powder averaging for the various methods. From the plots in Fig. 4, it is clearly evident that among the methods investigated, REPULSION provides the most uniform set of solid angles promising efficient and reliable numerical powder averaging using a minimum of different crystallite orientations.

Two criteria may be employed for numerical evaluation of the actual powder-averaging efficiency. First, the result of a computer simulation should ideally be invariant toward any rotation of the anisotropic tensor(s) prior to the powder averaging. Otherwise, the powder averaging may by itself introduce systematic errors being particularly severe when using powder methods for determination of magnitudes *and* relative orientation of tensors from several anisotropic interactions. Second, the discrepancy between any simulated spectrum and a totally converged spectrum should be as small as possible. The first convergence criterion is readily employed in praxis by calculating a series of spectra subjected to different (ideally uniformly distributed) reorientations of the anisotropic tensor(s) relative to the crystal-fixed coordinate system prior to the powder averaging. The distribution of spectra around an average spectrum, calculated as the normalized sum of all spectra, provides direct insight into the performance of the powder averaging. The second method, on the other hand, requires a totally converged spectrum, i.e., the ideal simulation or an analytical solution. However, this method has the important drawback that just through the selection of a single orientation of the tensor(s) relative to the crystal-fixed frame, it may introduce systematic preferences to one or more of the methods described above unless an extremely large number of crystallites is employed for the ideal spectrum and several spectra representing different tensor orientations are involved in the comparison. Therefore, this approach is only employed to ensure that the powder-averaging methods converge to a reasonable value.

Let the absolute difference Δ between two spectra S_1 and S_2 be defined as

$$\Delta(S_1, S_2) = \frac{1}{N_{\text{sig}}} \sum_{i=1}^{N_{\text{sig}}} |\text{Re}[S_1(i)] - \text{Re}[S_2(i)]|, \quad [10]$$

with N_{sig} denoting the number of points in the spectra. It is noted that Eq. [10] used the fact that solid-state NMR powder spectra involving static as well as rotating samples can be phased into pure absorption (here defined as the real part); for rotating samples, this requires averaging over the third Euler angle γ (*12*). Upon calculation of Q spectra with different orientation of the tensor(s) relative to the crystal-fixed coordinate system, it is useful to introduce the average of the differences to the average spectrum,

$$\bar{S} = \frac{1}{Q} \sum_{i=1}^{Q} S_i, \quad [11]$$

given by

$$\bar{\Delta} = \frac{1}{Q} \sum_{i=1}^{Q} \Delta(S_i, \bar{S}). \quad [12]$$

A measure for the quality of the powder averaging is now provided either directly by $\bar{\Delta}$ or by the standard deviation (Dev) of the Q Δ values relative to $\bar{\Delta}$:

$$\text{Dev}(\Delta) = \sqrt{\frac{1}{Q} \sum_{i=1}^{Q} (\bar{\Delta} - \Delta_i)^2}, \quad [13]$$

where we note that 95% of all Δ values should be found inside ± 2 Dev(Δ) around the average value.

Figure 5 gives a graphical representation of $\bar{\Delta}$ and Dev(Δ) values calculated for the various powder averaging methods using Eqs. [10]–[13] for $Q = 100$ MAS NMR spectra differing in the orientation of the anisotropic tensor relative to the crystal-frame being involved in the powder averaging. Specifically, each simulation represents an aniso-

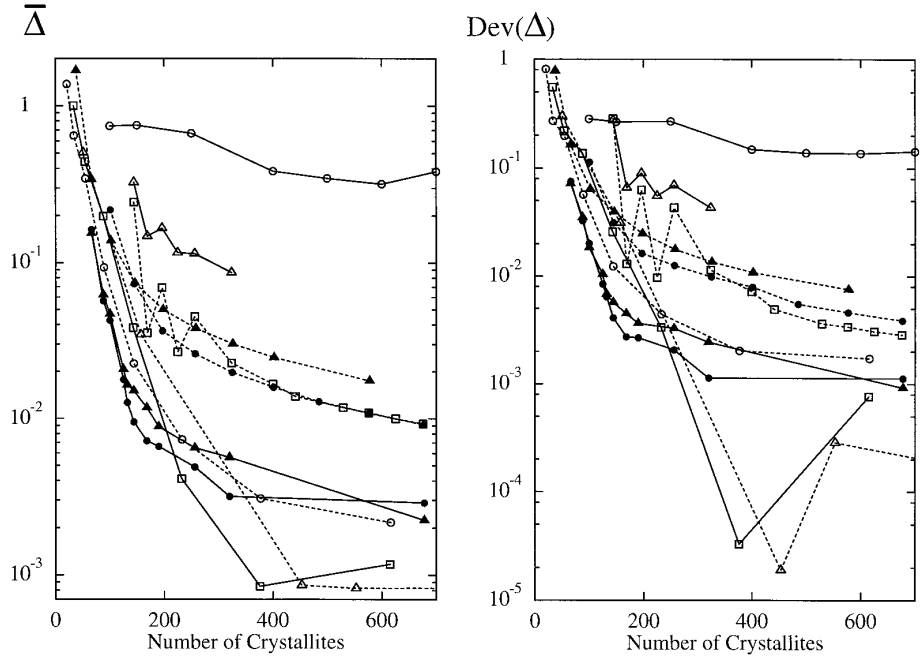

FIG. 5. Average absolute differences ($\bar{\Delta}$) and standard deviations of absolute differences [Dev(Δ)] calculated for the various powder-averaging methods on basis of $Q = 100$ ^{13}C chemical shielding anisotropy spectra differing in the orientation of the anisotropic tensor relative to the crystal-fixed frame. The spectra were calculated using parameters corresponding to the MAS NMR spectrum (1500 Hz spinning frequency) of the carbonyl group in zinc acetate recorded at a Larmor frequency of 80 MHz ($\omega^{iso}/2\pi = 0$, $\omega^{aniso}/2\pi = -6460$ Hz, and $\eta = 0.34$). The different tensor orientations were uniformly distributed over the sphere using the method in Appendix 1 with N = 100 (we note that random selection of these orientations leads to curves of very similar appearance). Specifically, the curves corresponds to random (—○—), planar grid (– – □ – –), spherical grid (—△—), planar ZCW (using g_1 and g_2 values corresponding to $f = \alpha^2\beta^2$) (—□—), spherical ZCW (using g_1 and g_2 values corresponding to $f = \alpha^2\beta^2$) (– – ○ – –), planar ZCW (4) (using g_1 and g_2 values corresponding to anisotropic chemical shielding of a static sample) (– – △ – –), Alderman (– – ● – –), SOPHE (with weighting factors calculated using Eq. [9]) (– – ▲ – –), REPULSION with unit area (—▲—), and REPULSION with weighting factors calculated using Eq. [9] (—●—).

tropic chemical shielding powder pattern corresponding to a ^{13}C MAS spectrum of the carbonyl group of zinc acetate recorded at a carbon resonance frequency of 80 MHz and using a spinning frequency of 1500 Hz. To avoid systematic errors, the $Q = 100$ different tensor orientations were uniformly distributed over the sphere using the REPULSION method. It should be mentioned, however, that calculations performed using 100 randomly selected tensor orientations essentially provided the same result. Clearly, the curves in Fig. 5 provide a very direct measure of the powder-averaging efficiency and the convergence of the various methods as function of the number of crystallites used for the powder averaging. We note that comparison of the simulated spectra with a simulation using 100,000 crystallites selected using the planar 2D grid method verifies that the curves in Fig. 5 converge to an reliable value upon increasing the number of crystallite orientations.

It is evident that the random crystallite method provides a very inefficient powder averaging. The 2D grid, SOPHE, and Alderman methods converge more rapidly, but generally require several hundreds of crystallites in order to achieve acceptable powder averaging. Clearly, the two most efficient schemes are the ZCW and REPULSION methods. Among these, REPULSION is superior when using a number of crystallites in the regime up to about 250. In the regime of 50–250 crystallite orientations, being extremely relevant for calculation of magic-angle-spinning (MAS) NMR spectra, it appears that for any acceptable standard deviation the REPULSION method provides a significant reduction in the number of required crystallite orientations as compared to earlier methods. At larger numbers of crystallites, the difference between REPULSION and the ZCW methods becomes insignificant, taking into account the logarithmic vertical scale, although it appears that the ZCW method provides slightly more efficient averaging than the REPULSION method. The latter observation may be ascribed to the fact that it is increasingly difficult to numerically obtain fully converged sets of REPULSION crystallite orientation with increasing number of crystallites.

Several other interesting features appear from Fig. 5. First, it surprisingly appears that the planar 2D grid and ZCW methods generally tend to converge faster than their spherical counterparts. Second, the planar ZCW partition schemes optimized to the $f = \alpha^2\beta^2$ and the anisotropic chemical shielding (static sample) functions behave very similar, indicating that this pow-

der-averaging scheme may be employed without concerning the specific function to be averaged. In practice, functional independence, being intrinsic in the REPULSION method, is of fundamental practical importance since the powder-averaging method otherwise may introduce systematic errors in iterative fitting of experimental spectra where the function may change by changing the parameters being fitted.

CONCLUSION

In conclusion, we have proposed and analyzed a new method (REPULSION) for efficient powder averaging in magnetic resonance using a minimum of crystallite orientations. Due to highly uniform sets of crystallite orientations, powder averaging using REPULSION converges faster than averaging using previous methods with respect to the number of crystallite orientations employed in the averaging. This may translate directly into reduced computation time required for simulation of powder spectra *but* also improves the reliability of parameters for the anisotropic interactions extracted from these through removal of systematic errors otherwise resulting from a nonuniform distribution of crystallite orientations. The advantage of the REPULSION method is particularly pronounced in the range of 50–250 different crystallite orientations, especially being relevant for simulation of MAS NMR spectra.

We note that by introducing simple symmetry constraints between the various octants of the unit sphere, it should be a straightforward matter to generate sets of REPULSION angles for smaller fractions of the unit sphere, being relevant for a variety of practical applications of powder averaging in solid-state NMR. Furthermore, the REPULSION method may potentially find application for generation of crystallite orientations, being suited for combination with efficient interpolation methods. Finally, we note that files including Euler angles and weighting factors for REPULSION partition schemes with different numbers of crystallites may be obtained from the authors upon request.

APPENDIX 1

Pseudo Computer Code for Iterative Determination of Uniformly Distributed Sets of Crystallite Orientations Using REPULSION

for i = 1 to N
  $\overrightarrow{OR}_i = \overrightarrow{OP}_i$ = random
end

do
  $\overrightarrow{dP}_{sum} = 0$
  for i = 1 **to** N
    for j = i + 1 **to** N
      $\vartheta_{ij} = \cos^{-1}(\overrightarrow{OP}_i \cdot \overrightarrow{OP}_j)$
      $\overrightarrow{V} = \overrightarrow{OP}_j \times \overrightarrow{OP}_i$
      $\overrightarrow{dP}_i = \overrightarrow{V} \times \overrightarrow{OP}_i$
      $\overrightarrow{OR}_i = \overrightarrow{OR}_i + C/\vartheta_{ij}^2 \cdot \overrightarrow{dP}_i / |\overrightarrow{dP}_i|$
      $\overrightarrow{OR}_i = \overrightarrow{OR}_i / |\overrightarrow{OR}_i|$
      $\overrightarrow{dP}_j = \overrightarrow{OP}_j \times \overrightarrow{V}$
      $\overrightarrow{OR}_j = \overrightarrow{OR}_j + C/\vartheta_{ij}^2 \cdot \overrightarrow{dP}_j / |\overrightarrow{dP}_j|$
      $\overrightarrow{OR}_j = \overrightarrow{OR}_j / |\overrightarrow{OR}_j|$
      $\overrightarrow{dP}_{sum} = \overrightarrow{dP}_{sum} + \overrightarrow{dP}_i + \overrightarrow{dP}_j$
    end
  end
  for i = 1 **to** N
    $\overrightarrow{OP}_i = \overrightarrow{OR}_i$
  end
while $\overrightarrow{dP}_{sum} \neq 0$

ACKNOWLEDGMENT

Support from Carlsbergfondet is acknowledged.

REFERENCES

1. D. W. Alderman, M. S. Solum, and D. M. Grant, *J. Chem. Phys.* **84,** 3717 (1986).
2. M. J. Mombourquette and J. A. Weil, *J. Magn. Reson.* **99,** 37 (1992).
3. L. Andreozzi, M. Giordano, and D. Leporini, *J. Magn. Reson. A* **104,** 166 (1993).
4. J. M. Koons, E. Hughes, H. M. Cho, and P. D. Ellis, *J. Magn. Reson. A* **114,** 12 (1995).
5. D. Wang, and G. R. Hanson, *J. Magn. Reson. A* **117,** 1 (1995).
6. H. W. Spiess, *in* ''NMR Basic Principles and Progress'' (P. Diehl, E. Fluck, and R. Kosfeld, Eds.), Vol. 15, Springer-Verlag, Berlin, 1978.
7. M. Mehring, ''Principles of High Resolution NMR of Solids,'' 2nd ed., Springer, New York, 1983.
8. S. K. Zaremba, *Ann. Mat. Pura Appl.* **4–73,** 293 (1966).
9. H. Conroy, *J. Chem. Phys.* **47,** 5307 (1967).
10. V. B. Cheng, H. H. Suzukawa, Jr., and M. Wolfsberg, *J. Chem. Phys.* **59,** 3992 (1973).
11. W. H. Press, S. A. Teukolsky, W. T. Vetterling, and B. P. Flannery, ''Numerical Recipes in C: The Art of Scientific Computing,'' 2nd ed., Cambridge Univ. Press, Cambridge, 1992.
12. M. H. Levitt, *J. Magn. Reson.* **82,** 427 (1989).